JOURNAL OF NANO- AND ELECTRONIC PHYSICS
Vol. **12** No 2, 02028(4pp) (2020)

ЖУРНАЛ НАНО- ТА ЕЛЕКТРОННОЇ ФІЗИКИ
Том **12** № 2, 02028(4cc) (2020)

Structural Properties of ($Ba_{0.97}Ca_{0.03}Ti_{0.985}Sn_{0.015}O_3$)-($K_{0.5}Na_{0.5}NbO_3$) Lead-free Electroceramics

Pravin S. Kadhane*, B.G. Baraskar, T.C. Darvade, R.C. Kambale†

Department of Physics, Savitribai Phule Pune University, Pune 411007, Maharashtra, India

(Received 15 February 2020; revised manuscript received 15 April 2020; published online 25 April 2020)

The lead-free $Ba_{0.97}Ca_{0.03}Ti_{0.985}Sn_{0.015}O_3$(BCTS)-$K_{0.5}Na_{0.5}NbO_3$ (KNN) (BCTS and BCTS + 1 wt. % KNN) electroceramics were synthesized by solid-state reaction and studied their structural, microstructural, dielectric, and ferroelectric properties. BCTS and BCTS + 1 wt. % KNN samples revealed the formation of perovskite structure without any trace of impurity. At room temperature, BCTS exhibits the tetragonal structure, while BCTS + 1 wt. % KNN shows an orthorhombic structure, which is evidenced by XRD and Raman spectroscopy study. Dense microstructure with average grain size of 1.75 μm and 1.67 μm, having bulk densities of 5.73 g/cm^3 and 5.48 g/cm^3 are observed for BCTS and BCTS + 1 wt. % KNN ceramics respectively. The dielectric study with respect to temperature depicts three polymorphic structural transitions corresponding to the rhombohedral to orthorhombic (T_{R-O}), orthorhombic to tetragonal (T_{O-T}) and tetragonal to cubic (T_C) structure. BCTS ceramic exhibited T_{R-O} at – 50 °C, T_{O-T} at 16 °C and T_{T-C} at 125 °C. P-E hysteresis loop at various temperatures provides information about the ferroelectric to paraelectric structural transition for BCTS ceramics and supports the temperature-dependent dielectric and Raman spectroscopy studies.

Keywords: Lead-free, $BaTiO_3$, Phase transition, Ferroelectrics, Curie temperature.

DOI: 10.21272/jnep.12(2).02028 PACS numbers: 74.62. – c, 77.22.Ej, 77.80.Bh, 77.84.Cg

1. INTRODUCTION

Currently, the inter-conversion of energy obtained from piezoelectric effect becomes an important task in electronics as well as defense departments for devices and applications. Verity of sensor's actuator's drug delivery systems printers and sonar's equipment are based on the piezoelectric effect [1-3]. Now a day's $PbZr_{1-x}Ti_xO_3$ (PZT) based materials play a crucial role in designing of these devices due to its high Curie temperatures and excellent ferroelectric/piezoelectric properties. Lead (Pb) in PZT is highly noxious and its toxicity increases during calcinations/sintering which causes enhancement in environmental pollution [4-7]. Thus, it becomes an open challenge to discover new lead free electroceramics for applications which can be replacing the use of PZT ceramics. Among the lead-free ferroelectric/piezoelectric materials, perovskite-structured such as $BaTiO_3$ [BT], $(Bi_{1/2}Na_{1/2})TiO_3$ [BNT], $(Bi_{1/2}K_{1/2})TiO_3$ [BKT], $KNbO_3$ [KN], $(KNa)NbO_3$ [KNN], drawn great importance to researchers [8-10]. Among all these, $BaTiO_3$ based materials show quite reliable and stable dielectric and ferroelectric properties. $BaTiO_3$ based piezoceramics have most important concern of low Curie temperature (Tc) ~ < 100 °C, results in temperature-dependent properties [11]. Thus, the motivation of this work is to modify the $BaTiO_3$ ceramics by Ca^{2+} at A site and Sn^{4+} at B site of ABO_3 perovskite structure with KNN addition in weight percent (wt. %) and investigate their structural transition with respect to temperature. The observed properties are discussed based on the structure-property relationship.

2. EXPERIMENTAL DETAILS

$Ba_{0.97}Ca_{0.03}Ti_{0.985}Sn_{0.015}O_3$ (BCTS) and $Ba_{0.97}Ca_{0.03}Ti_{0.985}Sn_{0.015}O_3$-$K_{0.5}Na_{0.5}NbO_3$ (BCTS + 1 wt. % KNN) electroceramics were separately prepared by conventional solid-state reaction. Barium carbonates ($BaCO_3$), calcium carbonate ($CaCO_3$), tin oxide (SnO_2), titanium dioxide (TiO_2), potassium carbonate (K_2CO_3), sodium carbonate (Na_2CO_3), niobium oxide (Nb_2O_5) (all with purity ≥ 99 % received from Sigma-Aldrich) were used as raw materials for synthesis of BCTS and BCTS + 1 wt. % KNN. Raw materials were weighed in their stoichiometric proportion followed by 24 h ball milling into ethanol medium. Then the mixture was dried at 80 °C overnight and grounded for 1 h. The pre-sintering of BCTS ceramic was done at 1100 °C for 10 h and that of KNN at 800 °C for 4 h. The pre-sintered powder is grounded further for 1 h and 1 wt. % KNN powder was added in parent BCTS composition for synthesis of BCTS + 1 wt. % KNN. Again BCTS and BCTS + 1 wt. % KNN milled in ethanol medium for 24 h then dried at 80 °C overnight. Pre-sintered powder was pelletized with 5 wt. % polyvinyl alcohol binder into 1 cm diameter pellets. The final sintering of prepared BCTS and BCTS + 1 wt. % KNN green ceramic were done at 1200 °C for 5 h.

The structural analysis was carried out by using X-ray powder diffraction (XRD) with CuKα radiation (λ = 1.5406 Å) (D8 Advanced, Bruker Inc., Germany). Temperature-dependent Raman measurements were performed using Raman spectroscopy (Renishaw In Via microscope Raman) with Linkam heating-cooling stage (THMS 600) in the range of 100 cm^{-1}-1000 cm^{-1} using a He-Ne laser of 532 nm line. The bulk density of the sample was determined using Archimedes principle in xylene medium. The microstructure was examined by scanning electron microscope (JEOL-JSM 6306A). The dielectric properties with respect to temperature were examined by using LCR meter (HIOKI 3532-50) at 100 kHz in temperature range of – 90 °C to 180 °C. Polarization verses electric field hysteresis loop was recorded at 50 Hz, using P-E loop tracer (Marine India).

* pravinkadhane89@gmail.com
† rckambale@gmail.com

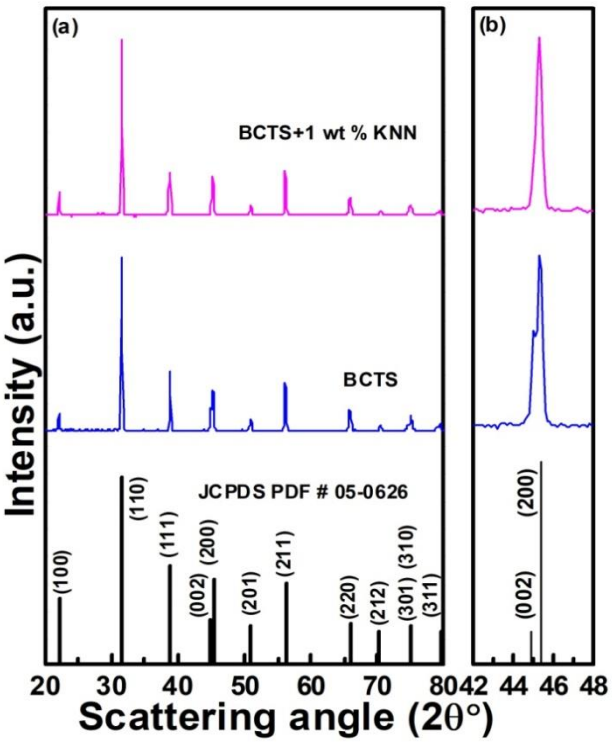

Fig. 1 – (a) X-ray diffraction pattern between 2θ range of 20°-80°, (b) enlarged range of 2θ = 42°-48° of BCTS and BCTS + 1 wt. % KNN electroceramics

3. RESULTS AND DISCUSION

Fig. 1a shows the XRD pattern of BCTS and BCTS + 1 wt. % KNN ceramic sintered at 1200 °C. All the observed XRD reflections are in good agreement with standard JCPDS (PDF # 05-0626) data which confirms the formation of pure perovskite phase without trace of any other secondary phase formation with space group P4mm. At room temperature BCTS possess tetragonal structure which is characterized by splitting of (002)/(200) peaks around 2θ = 45°. With the small wt. % addition of KNN in BCTS ceramic the structure changing from tetragonal to orthorhombic structure which is characterized by a single peak of (200) around 2θ of 45° as shown in Fig. 1b. Bulk density calculated by the Archimedes principle was found to be 5.73 gm/cm^3 and 5.48 gm/cm^3 for BCTS and BCTS + 1 wt. % KNN respectively. The microstructure of BCTS and BCTS + 1 wt. % KNN ceramics sintered at 1200 °C for 5 h are shown in Fig. 2a and Fig. 2b respectively. In accordance with bulk density measurements, dense microstructure with inhomogeneous grains distribution was observed. The average grain size calculated by line intercepts method is 1.75 μm and 1.67 μm for BCTS and BCTS + 1 wt. % KNN respectively [12]. Fig. 2c shows the dielectric constant (ε_r) and dielectric loss (tanδ) with respect to temperature for frequency 100 kHz in the temperature range from – 90 °C to 180 °C for BCTS composition. The BCTS ceramic is exhibit two ferroelectric to ferroelectric structural transitions of rhombohedral (R) to orthorhombic (O), orthorhombic (O) to tetragonal (T) and one ferroelectric to paraelectric structural transitions of tetragonal (T) to cubic (C). The observed structural transition temperature for the BCTS ceramics are T_{R-O} at – 50 °C, T_{O-T} at 16 °C and T_{T-C} at 125 °C. The experimental value of dielectric constant is 4366 and the corresponding dielectric loss is 0.02 at T_C. The ferroelectric to paraelectric structural transition temperature for BCTS ceramic observed at 125 °C, which is near about to reported value of Curie temperature 121 °C [13, 14].

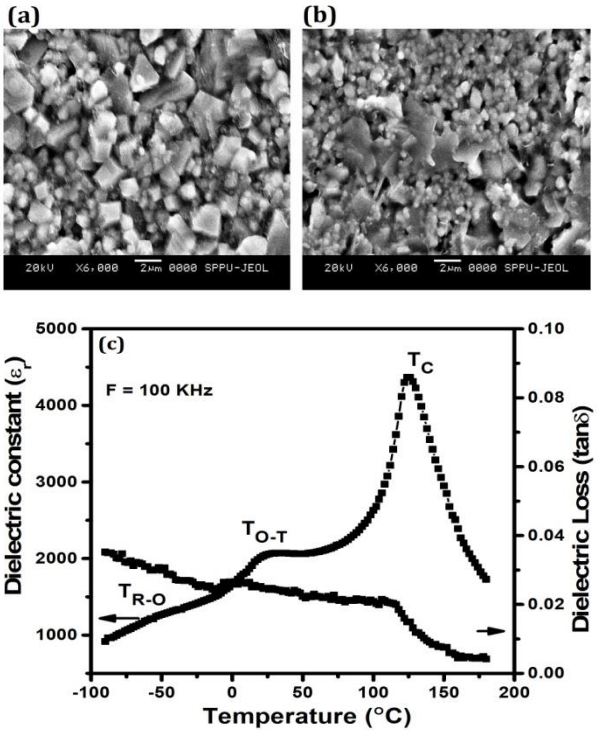

Fig. 2 – SEM micrograph of (a) BCTS, (b) BCTS + 1 wt. % KNN electroceramics, (c) temperature-dependent dielectric constant and dielectric loss of BCTS ceramic at a frequency of 100 kHz

Fig. 3a and Fig. 3b show the Raman spectra with respect to temperature for pure BCTS and BCTS + 1wt. % KNN ceramics respectively, which indicates the evolution of ferroelectric to ferroelectric and ferroelectric to paraelectric phase transformation. The Raman spectrum at – 100 °C shows the occurrence of the following Raman-active modes: v_3(LO), v_3(TO), v_4(LO), v_2(LO, TO), v_1(TO), and v_1(LO) situated around 168 cm^{-1}, 185 cm^{-1}, 225 cm^{-1}, 308 cm^{-1}, 525 cm^{-1}, and 715 cm^{-1}, respectively, which is significance of rhombohedral (R) phase, particularly the v_3(LO) peak at 168 cm^{-1} and two dips between v_3(LO) and v_3(TO) at 178 cm^{-1} as well as between v_3(TO) and v_4(LO) peaks at 194 cm^{-1}.

All Raman-active modes are in good agreement with those in the literature [15]. With increasing the temperature above – 50 °C, the rhombohedral phase characteristic peak v_3(LO) at 168 cm^{-1} disappears, while v_3(TO) and other peaks become broad, along with the disappearance of the dip between v_3(TO) and v_4(LO) peaks at 194 cm^{-1}. These results are the sign of phase structure of BCTS completely transforms into the orthorhombic (O) phase above – 50 °C. Further increasing temperature of BCTS near to 25 °C, the v_3(TO) peak at 180 cm^{-1} disappears, indicating that the phase structure changes from orthorhombic (O) to tetragonal (T) phase. In case of BCTS + 1 wt. % KNN at 25 °C, the v_3(TO) peak at 180 cm^{-1} is observed and it disappear at temperature 50 °C which indicates that this composition shows the

orthorhombic phase structure at room temperature which also have additional evidence from appearance of single peak (200) at $2\theta = 45°$in XRD pattern. Above the temperature 125 °C, v_1(LO) peak at 715 cm^{-1} and v_2(LO, TO) at 308 cm^{-1} are absent, and the whole spectrum gives only two broad peaks, v_1(LO) at 225 cm^{-1} and v_1(TO) at 525 cm^{-1}, indicates structural transition from tetragonal (T) to cubic (C) phase [16]. The temperature for phase transitions for R–O, O–T, and T–C is near – 50 °C, 25 °C, and 125 °C, respectively, which is consistent with the dielectric study.

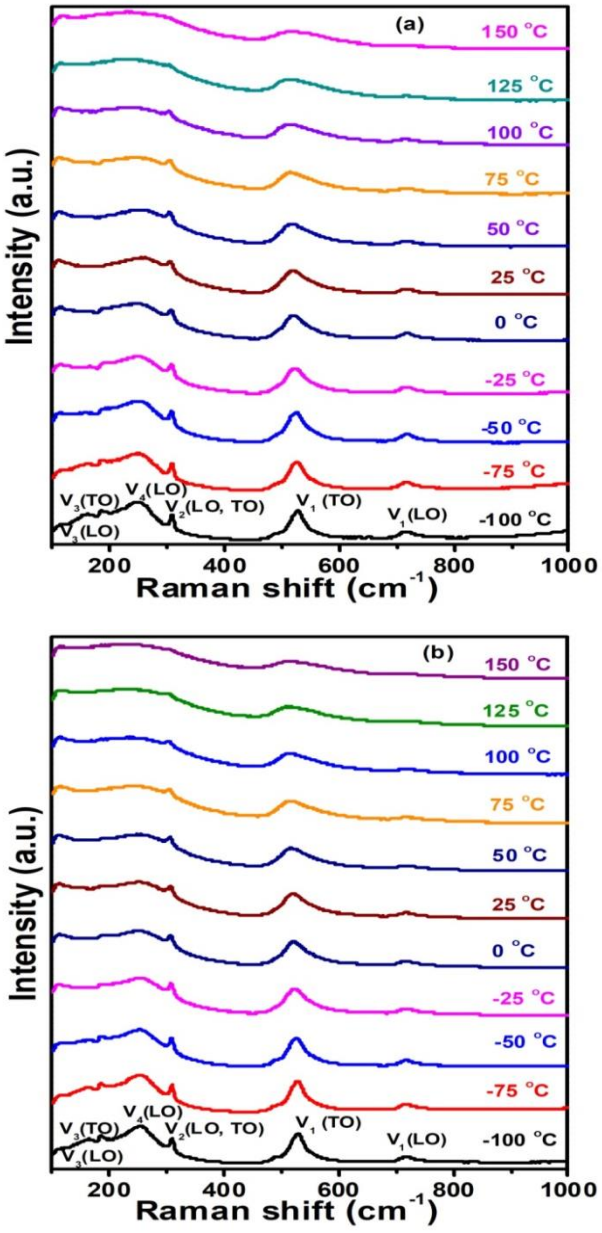

Fig. 3 – Raman spectra with respect to temperature for (a) BCTS and (b) BCTS + 1 wt. % KNN electroceramics in the temperature range of – 100 °C to 150 °C

Fig.4 shows the polarization verses electric field loop of BCTS ceramics, measured at temperature 30 °C, 60 °C, 90 °C, 120 °C, 150 °C. The temperature-dependent ferroelectric hysteresis loop is an intensive characterization technique to identify and confirm the structural change of material with respect to temperature. The nonlinear nature of the P-E loop up to the temperature 120 °C indicates the ferroelectric tetragonal structure while above this temperature it shows linear nature which indicates the paraelectric cubic structure for the BCTS composition. The values of the remnant polarization and coercive electric field with respect to temperature are approaches to zero as shown in Fig. 4e. This is an indication of phase transformation from the ferroelectric tetragonal phase to the paraelectric cubic phase above the temperature 125 °C [17, 18].Thus the temperature dependent P-E hysteresis measurement gives consistency with temperature-dependent dielectric constant and Raman spectroscopy study.

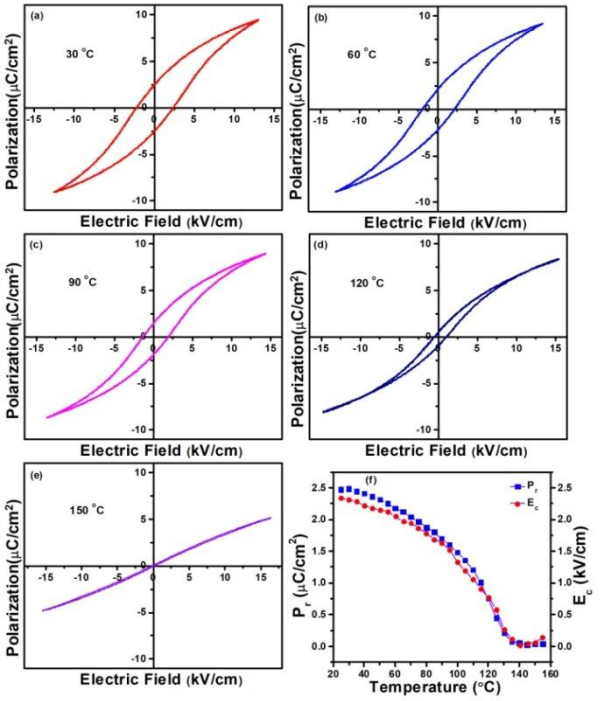

Fig. 4 – (a-e) Polarization versus electric field hysteresis loops: (a) 30 °C, (b) 60 °C, (c) 90 °C, (d) 120 °C, (e) 150 °C, (f) Remnant polarization and coercive electric filed with respect to temperature, for BCTS ceramic at a frequency of 50 Hz

4. CONCLUSIONS

$Ba_{0.97}Ca_{0.03}Ti_{0.985}Sn_{0.015}O_3$ (BCTS) and $Ba_{0.97}Ca_{0.03}Ti_{0.985}Sn_{0.015}O_3$-$K_{0.5}Na_{0.5}NbO_3$ (BCTS + 1 wt. % KNN) electroceramics were prepared by solid-state reaction. At room temperature, BCTS ceramic shows the tetragonal phase, while BCTS + 1 wt. % KNN shows an orthorhombic phase, which is evidenced by XRD and Raman spectroscopy study. P-E hysteresis loops at various temperatures provide information about the ferroelectric to paraelectric phase transition for BCTS electroceramics which is consistence with the temperature-dependent dielectric and Raman spectroscopy studies.

ACKNOWLEDGEMENTS

RCK thankfully acknowledge the Science and Engineering Research Board (SERB)-DST, Government of India (File No. EMR/2016/001750) for providing the research funds under the Extra Mural Research Funding (Individual Centric) scheme.

REFERENCES

1. J. Rödel, K.G. Webber, R. Dittmer, W. Jo, M. Kimura, D. Damjanovic, *J. Eur. Ceram. Soc.* **35**, 1659 (2015).
2. W. Liu, X. Ren, *Phys. Rev. Lett.* **103**, 257602 (2009).
3. P.K. Panda, B. Sahoo, *Ferroelectrics* **474**, 128 (2015).
4. M.D. Maeder, D. Damjanovic, N. Setter, *J Electroceram.* **13**, 385 (2004).
5. B.G. Baraskar, P.S. Kadhane, T.C. Darvade, A.R. James, R.C. Kambale, *Intechopen ferroelectric and their applications* 113 (2018).
6. S. Sagadevan, J. Podder, *J. Nano- Electron. Phys.* **7**, 04008 (2015).
7. S.G. Deshmukh, S.J. Patel, K.K. Patel, A.K. Panchol, V. Kheraj, *J. Electron. Mater.* **46**, 5582 (2017).
8. T. Takenaka, H. Nagata, *J. Eur. Ceram. Soc.* **25**, 2693 (2005).
9. T. Takenaka, H. Nagata, Y. Hiruma, *Jpn. J. Appl. Phys.* **55**, 01AA18 (2016).
10. T.R. Shrout, S.J. Zhang, *J.Electroceram.* **19**, 111 (2007).
11. J. Rödel, W. Jo, K.T.P. Seifert, E.M. Anton, T. Granzow, *J. Am. Ceram. Soc.* **92** [6], 1153 (2009).
12. E. Aksel, J.L. Jones, *Sensors* **10**, 1935 (2010).
13. W. Cai, Y. Fan, J. Gao, C. Fu, X. Deng, *J. mater. Sci. Mater electron* **22**, 265 (2011).
14. B.G. Baraskar, R.C. Kambale, A.R. James, M.L. Mahesh, C.V. Ramana, Y.D. Kolekar, *J. Am. Ceram. Soc.* **100**, 5755 (2017).
15. L.F. Zhu, B.P. Zhang, X.K. Zhao, L.Zhao, P.F. Zhou, J.F. Li, *J. Am. Ceram. Soc.* **96**, 241 (2013).
16. L.F. Zhu, B.P. Zhang, L. Zhao, J.F. Li, *J. Mater. Chem. C* **2**, 4764 (2014).
17. P.S. Kadhane, B.G. Baraskar, T.C. Darvade, A.R. James, R.C. Kambale, *Solid State Commun.* **306**, 113797 (2019).
18. P. Jaita, A. Watcharapasorn, N. Kumar, D.P. Cann, S. Jiansirisomboon, *Electron. Mater. Lett.* **11**, 828 (2015).